CHAPTER 10.15

Cementation

J. Brent Hiskey

Cementation is a general term used in the hydrometallurgical industry for the recovery of any dissolved metal from aqueous solution by contact reduction. More precisely, cementation or metal displacement is described as the electrochemical precipitation of a metal from solution by another more electropositive metal. The precipitation of copper on iron is a classic example of metal extraction by cementation:

$$Cu^{2+} + Fe^{\circ} \rightarrow Cu^{\circ} + Fe^{2+} \quad \textbf{(EQ 1)}$$

Cementation has been practiced since time immemorial. A process employing this reaction was successfully carried out by the ancient Chinese (Pu 1982; Lung 1986), and in the 17th century a license was granted by the Spanish Crown for the use of copper cementation on iron on a commercial scale at Rio Tinto, Spain (Nash 1912). Another classic example of the use of cementation in metal extraction is the recovery of gold from cyanide solution by zinc, which was part of the original MacArthur–Forrest process (MacArthur et al. 1887, 1889a, 1889b). Gold cementation onto zinc from cyanide solution was subsequently improved and is commonly known as the Merrill–Crowe process for gold recovery. For the most part, the early application of these processes was performed with limited understanding of the fundamental aspects of the reactions and of the role of important side reactions.

There are principally three areas of hydrometallurgy where cementation is used:

1. Primary metal recovery
2. Electrolyte purification
3. Treatment of dilute aqueous effluents

Prior to the advancements and adoption of modern techniques in copper solvent extraction and electrowinning, cementation accounted for the majority of the copper recovered from the leaching of low-grade ores in dumps and heaps throughout the world. One of the world's largest copper cementation plants was operated by Kennecott Utah Copper at the Bingham Canyon mine near Salt Lake City, Utah (United States). This facility was reviewed by Schlitt et al. (1979) and had two modules, each containing 13 large cone-type precipitators designed for producing 180 m/d of cement copper from low-grade copper leach solutions. This plant could handle a solution flow rate of 190 m^3/min.

Besides metal recovery, cementation is widely used for the purification of electrolytes. One important example is the removal of impurities in the electrolytic zinc process (EZP). This process accounts for approximately 90% of the world's zinc production. Contaminant ions such as cadmium, copper, nickel, and cobalt cause problems during zinc electrolysis and are removed from the electrolyte using zinc dust cementation.

Cementation is an extremely attractive method for removing hazardous metallic ions from process streams and effluents. Some examples include the precipitation of silver from photographic processing discharges, the cementation of cadmium by zinc in wastewaters, and the removal of mercury(II) from chloroalkali effluents using Zn and Fe.

The stoichiometry for a typical cementation reaction, as illustrated by Equation 1, is relatively simple, and the reaction kinetics frequently follow straightforward diffusion of the depositing ion to the surface of the substrate. In actuality, cementation is an extremely complex process, involving intricate interactions between electrochemical parameters and metal crystallization steps. Furthermore, the deposit structure and morphology can exhibit a significant effect on the overall efficiency of the process, and surface passivation often inhibits the reaction.

THERMODYNAMICS AND REACTION EQUILIBRIA

Cementation or contact reduction occurs between aqueous metal ions and a metal substrate according to the following general overall equation:

$$M_1^{z_1+} + \frac{z_1}{z_2} M_2^o = M_1^o + \frac{z_1}{z_2} M_2^{z_2+} \quad \textbf{(EQ 2)}$$

where $M_1^{z_1+}$ is the precipitating ion and M_2^o is the more electropositive metal surface. A rudimentary thermodynamic evaluation of the cementation reaction can be performed by a simple examination of the electromotive force series of the elements to determine which metal is more electropositive. A little more detail is provided by superimposing the respective oxidation potential–pH (Pourbaix) diagrams. This provides

J. Brent Hiskey, Professor Emeritus, Mining & Geological Engineering, University of Arizona, Tucson, Arizona, USA

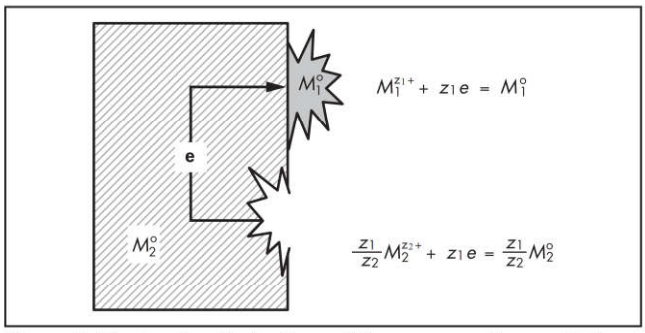

Figure 1 Electrochemical microcell for a general cementation reaction

a direct measure of the thermodynamic driving force for the reaction and the stable phases expected under mixed potential conditions. Ritchie (2003) explained this carefully for the Cu^{2+}/Zn system. Unfortunately, this approach does not predict the equilibrium concentrations of the individual metals.

The process is shown schematically in Figure 1 with separate half-cell reactions expressed as reduction steps. This is clearly an electrochemical system composed of two separate electron-transfer steps divided spatially from each other. These half-cell reactions when short-circuited represent a net cathodic process for the deposition of M_1^o and a net anodic process for the dissolution of M_2^o with electrons flowing from anode to cathode. The potential $E°$ for the short-circuited system at equilibrium is the same for both the cathode and the anode. Therefore, the respective Nernst reduction potentials become equal $E_{o1} = E_{o2}$, as expressed by the following equality:

$$E_{o1}^\circ + \frac{2.303\,RT}{z_1 F}\log a_{M_1^{z_1+}} = E_{o2}^\circ + \frac{2.303\,RT}{z_1 F}\log a_{M_2^{z_2+}}^{\frac{z_1}{z_2}} \quad \text{(EQ 3)}$$

where R is the molar gas constant, T is the absolute temperature, and F is the Faraday constant. From here it is possible to calculate the ratio of the activities of the metal ions under equilibrium conditions in the absence of complexing ligands. The corresponding ratio of $M_1^{z_1+}$ to $M_2^{z_2+}$ at 298 K is given by

$$\frac{(a_{M_1^{z_1+}})^{z_2}}{(a_{M_2^{z_2+}})^{z_1}} = \frac{[M_1^{z_1+}]^{z_2}}{[M_2^{z_2+}]^{z_1}} = 10^{\frac{-z_1 z_2 (E_{o1}^\circ - E_{o2}^\circ)}{0.059}} = \psi^{z_1 z_2} \quad \text{(EQ 4)}$$

where $[M_1^{z_1+}]$ and $[M_2^{z_2+}]$ represent the equilibrium concentrations of the metal ions for the corresponding cementation reaction, and Ψ is a function of ΔE_o°, the thermodynamic driving force and equals $10^{-\Delta E_o^o/0.059}$. From stoichiometry it follows that

$$[M_2^{z_2+}] = \frac{z_2}{z_1}([M_1^{z_1+}]_o - [M_1^{z_1+}]) \quad \text{(EQ 5)}$$

For many cementation systems (e.g., Cu^{2+}/Fe, Cu^{2+}/Zn), the equilibrium concentration $[M_1^{z_1+}]$ is much less than the initial concentration $[M_1^{z_1+}]_o$, therefore Equation 4 simplifies to the following relationship:

$$[M_1^{z_1+}] = \left(\frac{z_2}{z_1}[M_1^{z_1+}]_o\right)^{\frac{z_1}{z_2}} \psi^{z_1} \quad \text{(EQ 6)}$$

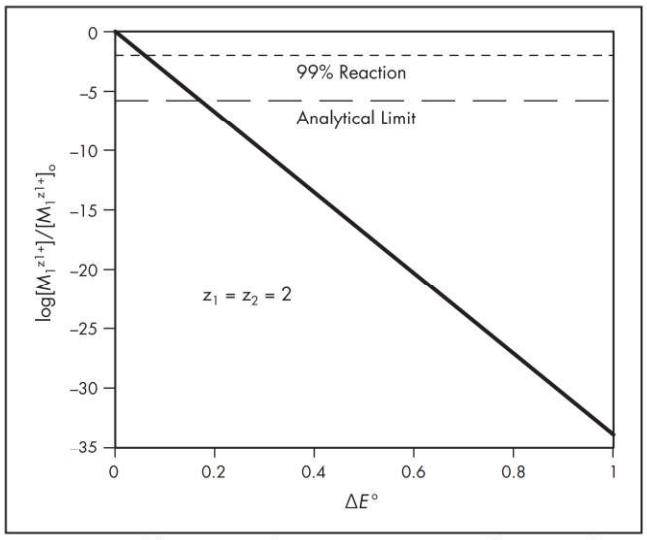

Figure 2 Equilibrium metal concentrations as a function of ΔE_o°

It is possible to calculate the ratio of $[M_1^{z_1+}]/[M_1^{z_1+}]_o$ for a select system at a given value of $[M_1^{z_1+}]_o$. A plot of $\log[M_1^{z_1+}]/[M_1^{z_1+}]_o$ as a function of ΔE_o° is shown in Figure 2. This figure was constructed for a hypothetical system where $z_1 = z_2 = 2$ and the value of $[M_1^{z_1+}]_o$ equals 0.001 M. As depicted in Figure 2, when the value of ΔE_o° increases, the equilibrium concentration of $M_1^{z_1+}$ moves to extremely low levels. In this figure, the top dashed line represents 99% reduction (for practical purposes, complete reduction) and even a small value of ΔE_o° equal to only 0.059 V corresponds to 99% reduction. Pang and Ritchie (1982) studied the mercury(I)–silver displacement reaction, which has an extremely low $\Delta E_o^\circ = -0.003$ V. Measurable reaction was observed at 298 K and $[Hg_2^{2+}] = 1.32 \times 10^{-2}$ M. When the value of ΔE_o° is greater than 0.2 V, the system comes to equilibrium below the analytical limit for dissolved metals. In actual systems, metal displacement falls short of the ideal theoretical equilibrium. For example, copper cementation on iron ($\Delta E_o^\circ = 0.777$ V) would have a predicted $\log[M_1^{z_1+}]/[M_1^{z_1+}]$ value equal to –26.34 at equilibrium. Experience has proven that the $\log[M_1^{z_1+}]/[M_1^{z_1+}]_o$ is seldom less than –3.0, even for extended cementation times. Several factors influence the final reactant concentration including surface passivation, caused by the formation of a stable second phase, and surface blockage by the depositing metal. In some cases, the formation of metal oxides and hydroxides can cause passivation (Ho and Ritchie 2002). Furthermore, when solubility limits are exceeded within the pore structure of the deposit, certain salts such as $FeSO_4$ (ferrous sulfate) can retard the reaction (Schalch et al. 1976).

A similar theoretical treatment can be performed for cementation systems containing metal complexes. For cementation processes involving metal complexes formed by type (L^-) ligands such as CN^- and Cl^-, the general overall stoichiometry follows this equation:

$$M_1(L)_\alpha^{(\alpha - z_1)-} + \frac{z_1}{z_2}M_2 = M_1 + M_2(L)_\beta^{(\beta - z_2)-} + \left(\alpha - \frac{z_1}{z_2}\beta\right)L^- \quad \text{(EQ 7)}$$

Table 1 Equilibrium concentration relationships for selected metal complex cementation systems

System	Equilibrium Concentration Relationship	ψ	K_α	K_β
$Au(CN)_2^-$ / Zn	$[Au(CN)_2^-] = \sqrt{[Au(CN)_2^-]_o}\frac{(K_\beta C_L^4+1)\psi}{\sqrt{2(K_\alpha C_L^2+1)}}$	1.72×10^{-42}	1.32×10^{39}	2.51×10^{31}
$Ag(CN)_3^{2-}$ / Zn	$[Ag(CN)_3^{2-}] = \sqrt{[Ag(CN)_3^{2-}]_o}\frac{(K_\beta C_L^4+1)\psi}{\sqrt{2(K_\alpha C_L^3+1)}}$	3.10×10^{-27}	2.08×10^{22}	2.51×10^{31}
$Cu(CN)_4^{3-}$ / Zn	$[Cu(CN)_4^{3-}] = \sqrt{[Cu(CN)_4^{3-}]_o}\frac{(K_\beta C_L^4+1)\psi}{\sqrt{2(K_\alpha C_L^4+1)}}$	1.87×10^{-22}	3.49×10^{30}	2.51×10^{31}

Note: The ψ, K_α, K_β values were calculated from HSC Chemistry software (Outotec 2009).

Several examples of practical importance that illustrate the role of complexation in cementation reactions are as follows:

$$Au(CN)_2^- + \tfrac{1}{2}Zn = Au + \tfrac{1}{2}Zn(CN)_4^{2-} \quad \textbf{(EQ 8)}$$

$$Ag(CN)_3^{2-} + \tfrac{1}{2}Zn = Ag + \tfrac{1}{2}Zn(CN)_4^{2-} + CN \quad \textbf{(EQ 9)}$$

$$Cu(CN)_4^{3-} = \tfrac{1}{2}Zn = Cu + \tfrac{1}{2}Zn(CN)_4^{2-} + 2CN \quad \textbf{(EQ 10)}$$

Sedzimir (2001) developed expressions analogous to Equation 6 for cementation equilibria comprising selected cyanide complexes. Table 1 presents relationships for the equilibrium concentrations of the depositing metal as a function of ligand concentration in stoichiometric excess.

The ratio of $\left[M_1(L)_\alpha^{(\alpha-z_1)-}\right]/\left[M_1(L)_\alpha^{(\alpha-z_1)-}\right]_o$ was calculated according to the relationships and data shown in Table 1 for the cementation of gold, silver, and copper from the respective cyanide complexes. These results are plotted in Figure 3 for $\log\left[M_1(L)_\alpha^{(\alpha-z_1)-}\right]/\left[M_1(L)_\alpha^{(\alpha-z_1)-}\right]_o$ as a function of $[CN^-]$.

These results exhibit very little sensitivity to cyanide concentration in the range shown. In general, the equilibrium concentration for metal complexes is greater than that for the free ions. It is not possible to compare this for the complexes of Au^+(aurous) and Cu^+(cuprous) ions since they are not thermodynamically stable in aqueous solution. They have a strong tendency of undergoing disproportionation. On the other hand, the equilibrium concentration of free Ag^+(argentous) ion cementation on zinc can be determined. The log $[Ag^+]/[Ag^+]_o$ would be about –24.7. Miller et al. (1990) examined the effect of [NaCN] on gold cementation from cyanide solution by particulate zinc. At 10^{-2} and 10^{-1} *M* NaCN the equilibrium gold concentration could have conceivably reached the analytical limit. At 10^{-3} *M* NaCN (sodium cyanide) the cementation reaction was retarded and log $[Au(CN)_2^-]/[Au(CN)_2^-]_o$ approached only –1.3. As observed by Barin et al. (1980), low cyanide ion concentrations inhibit the overall cementation reaction by the formation of $Zn(OH)_{2(solid)}$.

KINETICS

There is overwhelming empirical evidence that cementation reactions obey a first-order rate law. For an irreversible cementation reaction, the rate equation for surface area (A) and solution volume (V) is

$$\frac{d[M_1^{z_1+}]}{dt} = -\frac{k_o A}{V}[M_1^{z_1+}] \quad \textbf{(EQ 11)}$$

If the specific rate constant (k_o) is independent of concentration, the rate equation may be integrated to give the usual first-order form:

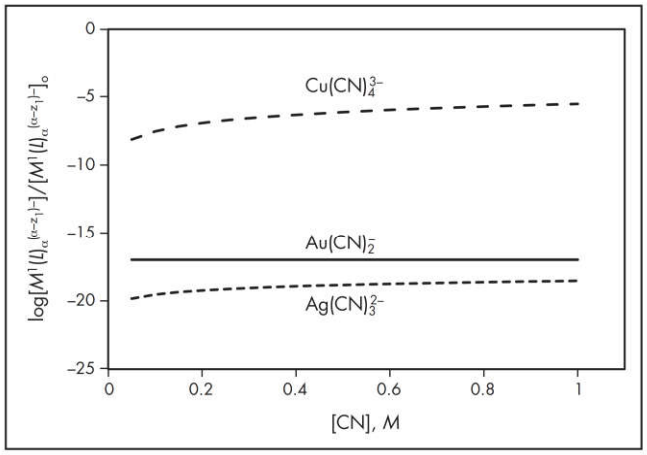

Figure 3 Initial and final metal complex concentrations as a function of cyanide concentration

$$\log\frac{[M_1^{z_1+}]}{[M_1^{z_1+}]_o} = -\frac{k_o A}{2.303\,V}t \quad \textbf{(EQ 12)}$$

where $[M_1^{z_1+}]_o$ and $[M_1^{z_1+}]$ equal the initial concentration and the concentration at time (t) of the noble metal ion. A plot of $\log[M_1^{z_1+}]/[M_1^{z_1+}]_o$ versus time would yield a straight line with a slope equal to $-(k_o A/2.303$ V) from which the value of (k_o) can be easily determined.

It can conveniently be shown that under conditions of boundary layer diffusion control that Equation 12 becomes

$$\log\frac{[M_1^{z_1+}]}{[M_1^{z_1+}]_o} = -\frac{A\,D}{2.303\,V\,\delta}t \quad \textbf{(EQ 13)}$$

where D is the coefficient of diffusion (cm^2/s) and δ is the boundary layer thickness (cm). It is apparent that k_o equals D/δ, which is identified as the apparent mass transfer coefficient. For cementation under strong agitation, the value of k_o would be of the order of 10^{-2} cm/s.

Evans Diagram

The mechanism of cementation reactions can be conveniently discussed in terms of Evans diagrams. Evans diagrams were originally applied as a graphical means for interpreting the rate of corrosion reactions (Bockris and Reddy 1973) and have been successfully adapted to the interpretation of cementation reactions. Power and Ritchie (1976) provided an excellent treatment of the use of Evans diagrams in the analysis of metal displacement (cementation) reactions. These diagrams

are basically the superimposition of the two independent current–potential (polarization) curves of the cementation constituent half reactions. Miller (1979) presented a thorough theoretical development and construction of a representative diagram. It is instructive to begin with the typical polarization curve for a general metal as shown in the log *i/E* plot in Figure 4. Three distinct regions are observed: at very low current densities, the potential is equal to the reversible electrode potential (E_o); at intermediate current densities, the potential varies linearly with log *i* (Tafel region); for sufficiently negative potentials, the current density assumes a maximum value (limiting current density) where diffusion to the electrode surface is controlling.

A characteristic Evans diagram for the cementation reaction between Cu^{2+} ions and Fe metal is depicted in Figure 5. This idealized diagram was constructed by Power and Ritchie (1976) from electrochemical data of Hurlen (1960, 1961). The anodic curve for iron dissolution is approximately a mirror image for that of copper deposition except diffusion is not typically observed until fairly high current densities are obtained.

The point of intersection of the two curves establishes the mixed potential for the cementation system. For this example, it indicates that the reaction is under mass transfer control. As shown, the mixed potential (E_m) for the conditions used in this plot is below the reversible potential for the copper electrode and the reaction should be under diffusion control. By contrast, the Evans diagram for the Fe^{2+}/Zn system (ΔE_o = 0.30 V) for 10^{-1} *M* Fe^{2+} reveals a point of intersection in the Tafel region and the rate would be expected to follow chemical control.

An idealized Evans diagram developed by Power (1975) and discussed by Miller (1979) clearly illustrates the point at which the cementation rate switches from mass transfer control to chemical control. The polarization diagram showing the shift from diffusion to chemical control is depicted in Figure 6.

As reasoned by Power (1975), cementation will likely be controlled by mass transfer when the equilibrium electrode potentials ($\Delta E_o = E_{o,c} - E_{o,a}$) of the component half-cell reactions differ by more than 0.36 V. It was also noted that if ΔE_o is less than 0.06 V, the system could be considered controlled by an electrochemical surface reaction. It is reasonable to accept that between these limits cementation will follow mixed kinetics. A simplifying assumption involves the use of the difference between the standard electrode potentials (ΔE_o°) for the component half-cell reactions as an approximation for ΔE_o.

Miller (1979) tabulated kinetic parameters for several cementation systems. Of the 15 systems listed, 13 had ΔE_o° values greater than 0.36 V, all of which exhibited rate constants and activation energies characteristic of diffusion control. The two systems for which $\Delta E_o^\circ < 0.36$ V, Ni^{2+}/Fe and Pb^{2+}/Fe, revealed activation energies typical of chemical control. Furthermore, the Ni^{2+} reduction by Fe exhibited a comparatively small rate constant of approximately 10^{-4} cm/s. Similar results were observed by Strickland and Lawson (1971, 1973).

It is important to recognize that, for various reasons, certain examples fail to conform to Evans diagram criterion. Annamalai and Hiskey (1978) examined the kinetics of copper cementation on aluminum. The Cu^{2+}/Al system has an extremely large ΔE_o° value equal to 2.04, which would certainly suggest diffusion control according to the Evans diagram. The naturally existing aluminum oxide film has a profound influence on the cementation reaction. The presence of chloride ion will attack the resistive oxide layer and allow copper cementation to occur. At temperatures <33°C, the experimental activation energy E_a = 20.4 kcal/mol which indicates reaction control for the system. This value is close to that obtained by MacKinnon and Ingraham (1970) for the same system (E_a = 14.7 kcal/mol at T < 40°C). Another example is the Cu^{2+}/Ni system where ΔE_o° = 0.57 V.

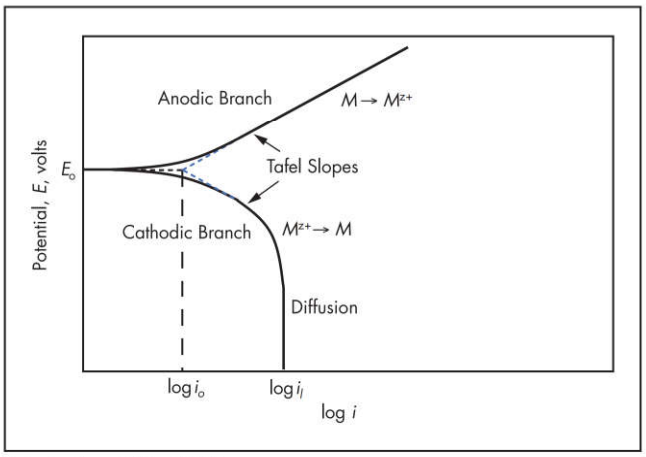

Adapted from Miller 1979

Figure 4 Typical polarization curves for a metal

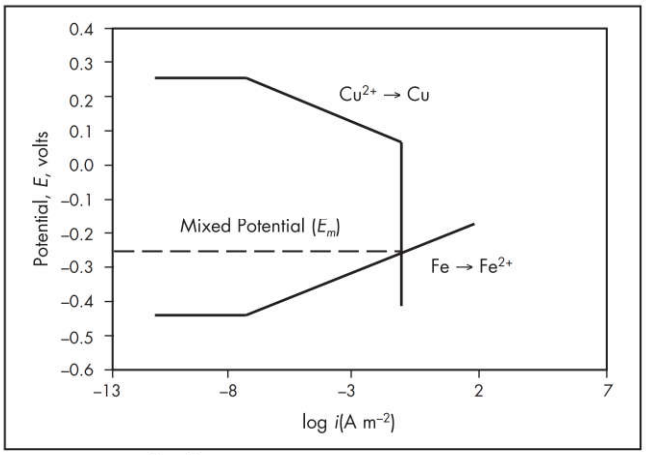

Source: Power and Ritchie 1976

Figure 5 Evans diagram for the Cu^{2+}/Fe system showing diffusion control. Polarization curves are for 10^{-3} *M* Cu^{2+} and Fe metal.

DEPOSIT STRUCTURE AND MORPHOLOGY

The crystal structure and morphological features of metal cementation deposits vary widely. Surface deposits have been observed to occur as powders, spongy clusters, fine and coarse dendrites, botryoidal groups, and uniform foil-like films. Metal deposits produced by cementation are similar to those formed during electrolytic deposition. This is certainly reasonable since both processes are electrochemical in nature. The physical characteristics of cementation surface deposits are influenced by such factors as hydrodynamic conditions, temperature, metal ion concentration, complexing ligands, and pH. Electrolytic deposits associated with electrorefining and electroplating are strongly dependent on current density

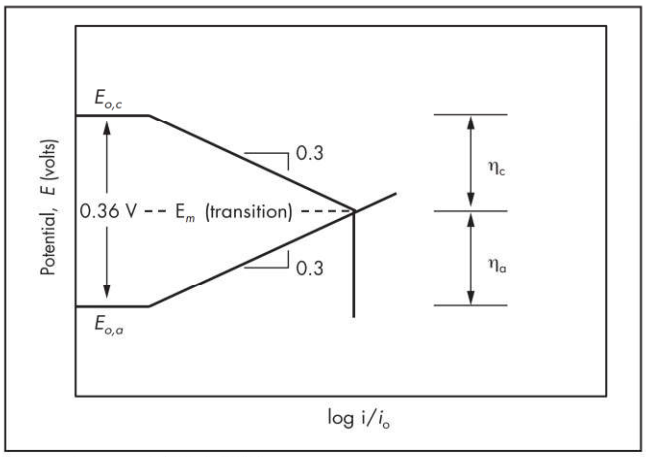

Source: Power and Ritchie 1976

Figure 6 Idealized Evans diagram showing the transition between diffusion and chemical control. Tafel slopes have been assumed to be 0.03 V per decade of log i/i_o and the exchange current densities are equal ($i_{o,c} = i_{o,a}$).

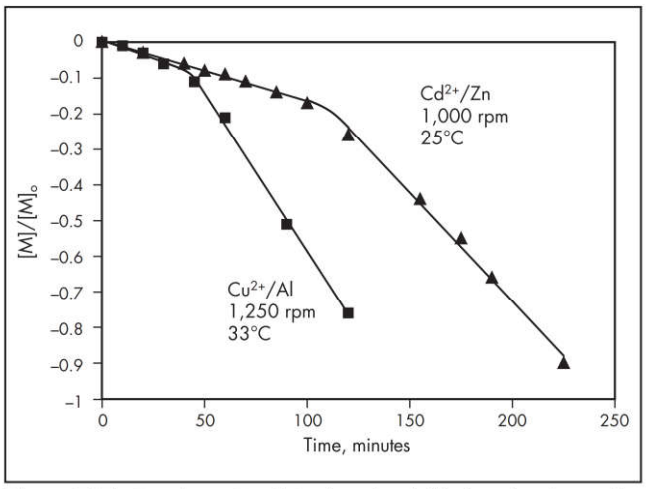

Figure 7 First-order rate plots showing initial and enhanced regions of cementation

and additives (i.e., smoothing agents). Current density is not an independent experimental or operational parameter for cementation reactions.

Deposit structure can have a pronounced effect on cementation kinetics. Some deposits can result in an enhancement of reaction rate while others can totally block the surface and severely retard the reaction. In many systems, two distinct kinetic regions are identifiable in the first-order rate plots. An initial slow period is followed by a second stage where the rate is noticeably enhanced. The initial stage is associated with deposition on a smooth surface and is relatively slow. As the deposit increases in thickness, surface roughness is developed. Surface features protrude into the boundary layer and cause localized turbulence that increases the mass transfer rate. Strickland and Lawson (1971) have discussed this in detail. They suggest that the enhanced rates are a result of surface roughness and/or an increase in the cathodic surface area.

First-order rate plots showing the initial and enhanced regions for cementation on rotating disks are provided in Figure 7 for the Cu^{2+}/Al and Cd^{2+}/Zn systems. Values of the specific rate constant k_o are presented in Table 2 for the initial and enhanced stages for the data shown in Figure 7.

Table 2 Values of the specific rate constant k_o

	Mass Transfer Coefficient, cm/s	
Cementation System	**Initial Stage**	**Enhanced Stage**
Cu^{2+}/Al	7.8×10^{-3}	3.5×10^{-2}
Cd^{2+}/Zn	6.4×10^{-3}	2.3×10^{-3}

Kinetic enhancements corresponding to 4.5 and 3.6 times for Cu^{2+}/Al and Cd^{2+}/Zn, respectively, were found for these systems. Strickland and Lawson (1971) have reported various degrees of enhancement ranging from 2 to 7 times for Cu^{2+}/Zn, Cu^{2+}/Fe, Pb^{2+}/Zn, Ag^{+}/Zn, Ag^{+}/Cu, and Ag^{+}/Cd in sulfate solutions.

Some cementation systems exhibit surface blockage by the deposit. This results in passivation of the surface and restriction of the anodic half-cell reaction. This can occur when the surface is covered by a massively heavy type of deposit that impedes diffusion within the pores of the deposit. Alternately, deposits that are dense, compact, and adherent can essentially block the reaction. There are many examples where surface blockage has affected the rate of the cementation reaction. Under certain conditions, cementation from cyanide solutions has demonstrated a propensity for blockage-type deposits. Ritchie (2003) has listed some general factors favoring surface blockage:

- Deposition from a complex ion
- When the reactant concentration exceeds some critical value
- Low reaction temperature
- Compatible structures for depositing and displacing metals

Von Hahn and Ingraham (1966) investigated the cementation of silver on copper in perchloric acid and alkaline cyanide solutions. For rotating disk geometry, they found kinetic enhancement in the perchloric acid system and a deposit structure that was composed of loosely adhering powder. On the other hand, in the alkaline cyanide system, silver cementation was inhibited by the deposit, which was smooth, dense, and strongly adherent.

ALLOY FORMATION

An interesting phenomenon associated with certain cementation reactions is the formation of metal alloys. This is especially interesting since cementation is carried out at relatively low temperatures (approximately room temperature). The theoretical and practical considerations involving the electrodeposition of alloys from aqueous solution have been examined for many years. Two classic examples are the electrolytic deposition of brass and bronze alloys. Brenner (1963) presented a considerable amount of information regarding the electrodeposition of alloys and reviewed an extensive list of examples. A limited number of alloys are formed during the electroless plating. The formation of alloys during cementation is even rarer.

One of the first investigations to observe alloy formation during cementation was that by Straumanis and Fang (1951). They studied deposits associated with the displacement of Cu, Au, Ni, and Ag on Zn. Copper deposits contained 9–13 at. %

Zn and were confirmed by the X-ray patterns to be α-brass. Annealing the deposit at 900°C resulted in sharp X-ray lines for α-brass and an increase in Zn content. Von Hahn and Ingraham (1966) examined the Pd^{2+}/Cu system and by X-ray-diffraction data clearly established the formation of Cu-Pd alloys and not pure Pd. The individual alloy crystallites of Cu-Pd ranged from 20 to 45 at. % Pd. Lee and Hiskey (2003) and Hiskey and Lee (2003) detected Au-Cu alloys during the cementation of gold on copper from ammoniacal thiosulfate solutions. The alloy composition was dependent on the initial Cu–Au ratio in solution. Intermetallic alloys were predominantly Cu_3Au in composition. Underpotential deposition theory is a possible mechanism for explaining the formation of these alloys.

LABORATORY EXPERIMENTS

Conceivably there are many experimental methods that might be used to investigate cementation reactions. Most investigations are aimed at obtaining kinetic and mechanistic data, and information about the efficiency of the reaction. This information is helpful in developing a chemical model for the system and in process scale-up. All studies basically depend on the type of reactor and the nature of the substrate. The two most common methods are performed in batch reactors using either suspended particles or a controlled geometry metallic substrate. Both systems can independently study such parameters as temperature, noble metal ion concentration, pH, ionic strength, complexing ligands, additives, and hydrodynamics.

Particulate System

A stirred batch reactor is typically used to suspend particles of different size in the solution. Particles are normally screened into narrow size fractions, and the geometric mean size for each particle size interval is used to calculate the total surface area. The particulate sample can be treated to remove oxide films and other debris from the surface prior to being introduced into the reactor. Solutions containing the noble metal ion are adjusted to the proper experimental conditions, and the experiment commences when the particles are added to the reactor. Agitation can be briefly stopped at set intervals to allow particles to settle and solution aliquots to be removed to analyze for the dissolved metal. In a suspension of spherical particles, it is possible to correlate the mass transfer coefficient to the agitation intensity according to the Harriott (1962) relationship.

Controlled Geometry

Most often, fundamental kinetic and mechanistic studies of cementation employ controlled geometry experiments. In this system, once again, batch cementation tests are carried out using metal strips under static conditions or a rotating disc or rotating cylinder apparatus. Rotating disc and cylinder systems create more agitation and thus reduce the diffusion boundary layer thickness. A disc geometry is very popular, not only because of simple fabrication, but importantly, the hydrodynamics of the system can be analyzed and modeled mathematically (Levich 1962). A rotating disc can be conveniently used to analyze the effect of surface roughness on the cementation reaction. Furthermore, electrochemical measurements using a rotating disc electrode assembly can be correlated directly to the rotating disc kinetic data. Another important feature of the rotating disc is the direct transfer of the disc for surface product examination by optical and scanning electron microscopy techniques. Prior to use, metal discs are polished using a successively finer grit size of silicon carbide paper. After thoroughly washing and rinsing, the disc is immersed into the test solution to start the reaction. Solution aliquots are periodically moved to analyze for the dissolved metal.

INDUSTRIAL APPLICATIONS OF METALLURGICAL CEMENTATION

As noted earlier, there are three main areas of hydrometallurgy where cementation is of industrial importance: primary metal recovery, electrolyte purification, and the treatment of dilute aqueous effluents. It should be emphasized that the general thermodynamic, kinetic, and electrochemical principles apply irrespective of application and method.

Metal Recovery

Copper

The cementation of copper on iron has been practiced for millennia with very little change to the basic operating principles. At Rio Tinto, Spain, copper cementation was outlined in the patent or license granted to Don Alvaro Alonso de Garfias in 1661 by the Spanish Crown; however, the installation of an engineered system was not achieved until 1752 (Nash 1904). The process employed channels (launders) and tanks loaded with iron sheets or scrap. During these early periods, relatively high-quality copper was produced at Rio Tinto: the poorest grade, *cobre negro*, contained about 90% Cu; and the finest grade, *cobre fino*, about 98% Cu. These precipitates were equal in quality to that obtained by smelting. In 1850, a smelter was constructed for the specific purpose of refining *cobre negro* precipitates.

Gravity-flow launders charged with shredded scrap iron remained the industrial standard for copper cementation plants associated with heap and dump leaching operations even into the 1980s. Spedden et al. (1966) indicate that processing 3,785 L/min of copper-bearing leach solution would require a launder section measuring 152.4 m long, 1.2 m wide, and 1.2 m deep. A large leaching operation would require several sections. A typical plant would also need the necessary pumping system, holding tanks, gantry or crane, trammel screens, thickeners, and drying pans. One variation used perforated plastic pipes positioned in the launder floor to evenly distribute pregnant leach solution (PLS) on the iron substrate. The normal operating cycle would consist of the following steps (Jacky 1967):

1. Bedding the section with iron
2. Introducing and controlling the PLS
3. Draining, washing, and excavating the copper precipitates
4. Washing the section and punching orifices

This system would effectively yield 90% copper recovery. These plants were relatively simple to construct and operate. Unfortunately, they suffered from poor hydrodynamics, high iron factors (2 to 4 times theoretical), a lot of manual labor, and impure copper precipitates that required additional refining. In an attempt to overcome some of the drawbacks of conventional launders, Kennecott designed a cone-type precipitator that was installed at their operations in the late 1960s. Figure 8 shows an illustration of a cone precipitator. A variation of this cementation reactor was developed by Kennecott that utilized sponge iron or particulate iron as the precipitant instead of shredded iron scrap (Back 1967).

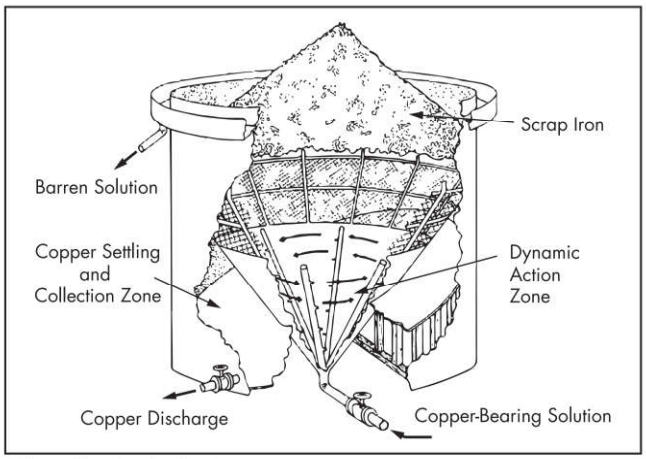

Adapted from Back 1967

Figure 8 Pictorial representation of Kennecott cone precipitator

Copper cementation was eventually phased out at most leaching operations with the successful development and implementation of copper solvent extraction (Hiskey 2014).

Gold

The cementation of gold by zinc was an integral part of the cyanide process as developed by MacArthur et al. (1887, 1889a, 1889b). Process improvements to the cementation unit operation are generally known today as the Merrill–Crowe process for gold recovery. The overall reaction for this process is shown in the following equation:

$$Au(CN)_2^- + \tfrac{1}{2}Zn = Au + \tfrac{1}{2}Zn(CN)_4^{2-} \quad \textbf{(EQ 14)}$$

The Merrill–Crowe cementation process is mainly employed for gold/silver recovery from dilute sodium cyanide solutions and is the preferred recovery method for gold cyanide solutions containing high silver concentrations. In addition, Merrill–Crowe is a process alternative to electrowinning for gold recovery from carbon-in-column and carbon-in-pulp eluates. A simplified process flow sheet is depicted in Figure 9.

For efficient precipitation, it is critical that the PLS be perfectly free of all suspended solids. This is normally accomplished by clarifying filters. Following clarification, the solution undergoes deaeration under vacuum to remove dissolved oxygen. Without this step there would be excessive zinc consumption during the cementation reaction. A properly operated deaeration tower can produce solution with <1 ppm O_2. Zinc dust is added along with barren cyanide solution to a small mixing cone. The zinc dust slurry is then combined with the clarified, deaerated PLS and the cementation reaction is initiated. This is followed by a plate-and-frame filter press where the cementation reaction is allowed to continue and the precipitated metals collected. A continuous cementation process will have several filter presses operating in parallel. Chi et al. (1997) reported that a typical cycle requires five to seven days for completion. At the end of each cycle, the filter cake is blown dry with air and then discharged for subsequent furnace refining. Depending on gold and sodium cyanide concentration, controlled additions of lead nitrate can serve as an activator or accelerator for the cementation reaction.

Electrolyte Purification—Electrolytic Zinc Process

The removal of trace levels of impurities from zinc sulfate electrolyte by cementation is a critical step in zinc electrowinning. Metals more electropositive than zinc (e.g., copper, nickel, cobalt, and cadmium) can exhibit detrimental effects during electrowinning, including co-deposition and redissolution of the cathode. These effects decrease current efficiency and result in poor product quality. Cementation of impurities by zinc dust has been an electrolyte purification strategy for many years. Important zinc does not add any impurities ions into the electrolyte. Metal cations are precipitated according to the following general reaction:

$$M^{2+} + Zn^o \rightarrow M^o + Fe^{2+} \quad \textbf{(EQ 15)}$$

Raghavan et al. (1999) reviewed several zinc dust purification technologies for various EZP producers in the world. The cold–hot purification method is a common approach in many plants. This treatment option is shown schematically in Figure 10.

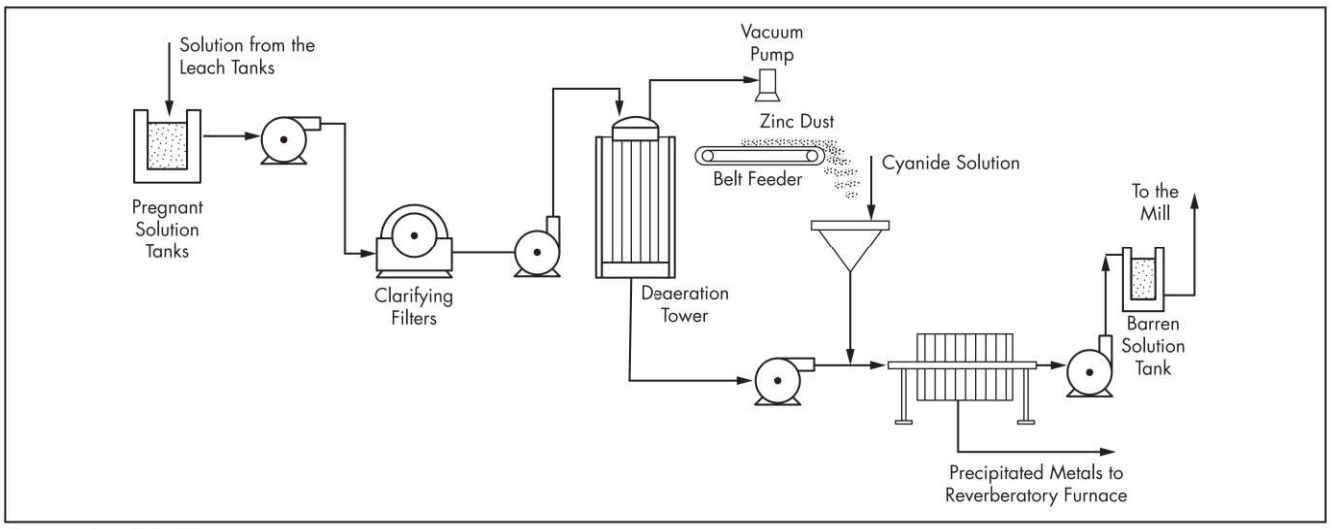

Source: Chi et al. 1997

Figure 9 Generalized flow sheet for gold/silver recovery by Merrill–Crowe cementation

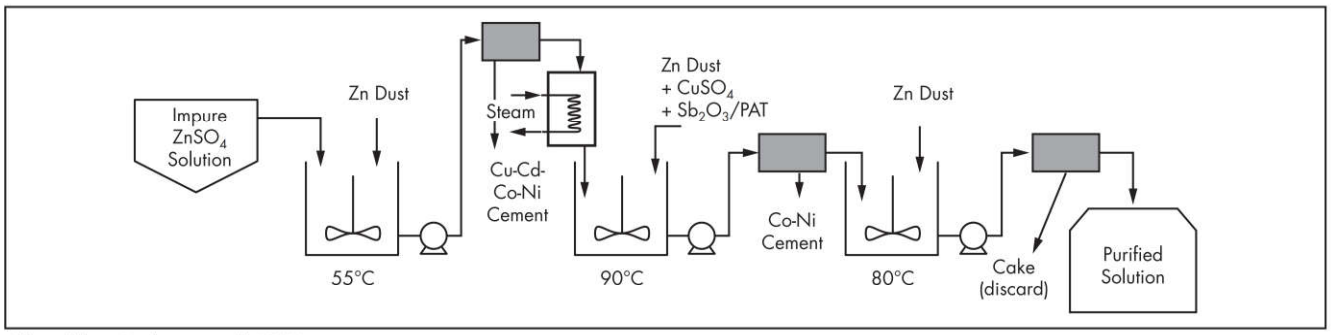

Adapted from Raghavan et al. 1999

Figure 10 Cold–hot EZP electrolyte purification method

More recently, Krause (2014) provided a comprehensive study aimed at optimizing the zinc cementation purification process. It was noted that a typical cold–hot purification scheme involves initial removal of copper at low temperature (60°–65°C), followed by high-temperature (70°–100°C) removal of cobalt and nickel using activators, and a final low-temperature (60°–65°C) cadmium cementation step. Because of slow cementation kinetics with cobalt and nickel, activators such as As_2O_3 (arsenic(III) oxide), Sb_2O_3 (antimony(III) oxide), antimony metal, or potassium antimony tartrate (PAT) are required (Singh 1996).

Treatment of Dilute Aqueous Effluents

Cementation is one of the most effective and economic techniques for removing toxic and dilute metal values from industrial waste solutions. It has been demonstrated to be a feasible technique because of its relative simplicity, ease of control, low energy consumption, and the ability to recover valuable metals and to stabilize toxic materials. Most of the initial interest was directed at waste streams containing dilute concentrations of copper. This was sensible given the extremely long history and operating experience using this technique for primary metal recovery. More recently, there as has been considerable interest in the treatment of effluents containing toxic heavy metals such as cadmium. The cementation of cadmium on zinc has been extensively studied in the laboratory (Younesi et al. 2006; Nosier 2003; Taha and Ghani 2005; Aurousseau et al. 2004). As early as 1975, Richard and Brookman (1975) proposed the use of cementation for the removal of mercury from wastewaters. Mercury removal from aqueous solution by zinc cementation has been an ongoing area of research (Ku et al. 2002).

REFERENCES

Annamalai, V., and Hiskey, J.B. 1978. A kinetic study of copper cementation on pure aluminum. *Min. Eng.* (June):650.

Aurousseau, M., Pham, N.T., and Ozil, P. 2004. Effects of ultrasound on the electrochemical cementation of cadmium by zinc powder. *Ultrason Sonochem*. 11(1):23.

Back, A.E. 1967. Precipitation of copper from dilute solutions using particulate iron. *J. Met.* (May):27.

Barin, I., Barth, H., and Yaman, A. 1980. Electrochemical investigation of the kinetics of gold cementation by zinc from cyanide solutions. *Erzmetallurgy* 33:399.

Bockris, J.O'M., and Reddy, A.K.N. 1973. *Modern Electrochemistry*. Vol. 2. New York: Plenum Press.

Brenner, A. 1963. *Electrodeposition of Alloys: Principles and Practice*. New York: Academic Press.

Chi, G., Fuerstenau, M.C., and Anderson, P.A. 1997. Study of Merrill–Crowe processing. Part II: Regression analysis of plant operating data. *Int. J. Miner. Process.* 49:185.

Harriott, P. 1962. Mass transfer to particles: Part I. Suspended in agitated tanks. *AIChE J*. 8(1):93–102.

Hiskey, J.B. 2014. Innovative strategies for copper hydrometallurgy. In *Mineral Processing and Extractive Metallurgy: 100 Years of Innovation.* Edited by C.G. Anderson, R.C. Dunne, and J.L. Uhrie. Englewood, CO: SME.

Hiskey, J.B., and Lee, J. 2003. Kinetics of gold cementation on copper in ammoniacal thiosulfate solutions. *Hydrometallurgy* 69:45.

Ho, E.M., and Ritchie, I.M. 2002. Cementation of copper ions by nickel metal. Paper presented at the Fifth International Symposium on Electrochemistry in Mineral and Metal Processing. The Electrochemical Society.

Hurlen, T. 1960. Electrochemical behavior of iron. *Acta Chem. Scand*. 14:1533.

Hurlen, T. 1961. On the kinetics of the Cu/Cu^{2+}_{aq} electrode. *Acta Chem. Scand*. 15:630.

Jacky, H.W. 1967. Copper precipitation methods at Weed Heights. *J. Met.* (April):22.

Krause, B.J. 2014. Optimisation of the purification process of a zinc sulfate leach solution for zinc electrowinning. M.E. thesis, Department of Materials Science and Metallurgical Engineering, University of Pretoria, South Africa.

Ku, Y., Wu, M.H., and Shen, Y.S. 2002. Mercury removal from aqueous solutions by zinc cementation. *Waste Manage.* 22:721–726.

Lee, J., and Hiskey, J.B. 2003. Alloy formation during the cementation of gold on copper from ammoniacal thiosulfate solutions. In *Hydrometallurgy 2003—Fifth International Conference in Honor of Professor Ian Ritchie –Volume 2: Electrometallurgy and Environmental Hydrometallurgy*. Edited by C.A. Young. Warrendale, PA: The Minerals, Metals & Materials Society.

Levich, V.G. 1962. *Physicochemical Hydrodynamics*. Englewood Cliffs, NJ: Prentice-Hall.

Lung, T.N. 1986. The history of copper cementation on iron—The world's first hydrometallurgical process from medieval China. *Hydrometallurgy* 17:113.

MacArthur, J.S., Forrest, R.W., and Forrest, W. 1887. Process of obtaining gold and silver from ores. British Patent 14,174.

MacArthur, J.S., Forrest, R.W., and Forrest, W. 1889a. Process of obtaining gold and silver from ores. U.S. Patent 403,202.

MacArthur, J.S., Forrest, R.W., and Forrest, W. 1889b. Process of separating gold and silver from ores. U.S. Patent 418,137.

MacKinnon, D.J., and Ingraham, T.R. 1970, Kinetics of copper (II) cementation on pure aluminum disc in acidic sulfate solutions. *Can. Metall. Q*. 9:443.

Miller, J.D. 1979. Cementation. In *Rate Processes of Extractive Metallurgy.* Edited by H.Y. Sohn and M.E. Wadsworth. New York: Plenum Press.

Miller, J.D., Wan, R.Y., and Parga, J.R. 1990. Characterization and electrochemical analysis of gold cementation from alkaline cyanide solution by suspended zinc particles. *Hydrometallurgy* 24:373.

Nash, W.G. 1904. *The Rio Tinto mine: Its history and romance*. London: Simpkin, Marshall, Hamilton, Kent.

Nash, W.G. 1912. Precipitation of copper from mine waters. *Min. Sci. Press* 104(5):212.

Nosier, S.A. 2003. Removal of cadmium ions from industrial wastewater by cementation. *Chem. Biochem. Eng. Q.* 17(3):219.

Outotec. 2009. HSC Chemistry software, version 7.0. Outotec.

Pang, J.T.T., and Ritchie, I.M. 1982. The reaction between mercury ions and silver: Dissolution and displacements. *Electrochim. Acta* 27(6):683.

Power, G.P. 1975. Cementation reactions. Ph.D. thesis, University of Western Australia, Perth, Western Australia.

Power, G.P., and Ritchie, I.M. 1976. A contribution to the theory of cementation (metal displacement) reactions. *Aust. J. Chem.* 29:699.

Pu, Y.D. 1982. The history and present status of practice and research work on solution mining in China. In *Interfacing Technologies in Solution Mining*. Edited by J.W. Schlitt and J.B. Hiskey. Littleton, CO: SME-AIME.

Raghavan, R., Mohanan, P.K., and Verma, S.K. 1999. Modified zinc sulphate solution purification technique to obtain low levels of cobalt for the zinc electrowinning process. *Hydrometallurgy* 51:187.

Richard, M.D., and Brookman, G. 1975. The removal of mercury from industrial waste waters by metal reduction. *Eng. Bull. Purdue Univ.* II, 713.

Ritchie, I.M. 2003. Some aspects of cementation reactions. In *Hydrometallurgy 2003—Fifth International Conference in Honor of Professor Ian Ritchie—Volume 2: Electrometallurgy and Environmental Hydrometallurgy*. Edited by C.A. Young. Warrendale, PA: The Minerals, Metals & Materials Society.

Schalch, E., Nicol, M.J., Balestra, P.E.L., and Stapleton, W.M. 1976. *An Electrochemical Investigation of Copper Cementation on Iron.* NIM Report No. 1799. Johannesburg: National Institute of Metallurgy.

Schlitt, W.J., Ream, B.P., Haug, L.J., and Southard, W.D. 1979. Precipitating and drying cement copper at Kennecott's Bingham Canyon facility. *Min. Eng*. (June):671.

Sedzimir, J. 2001. Precipitation of metals by metals (cementation) equilibria in absence or in presence of complexes in the solution. *Arch. Metall.* 46(1):3.

Singh, V. 1996. Technological innovation in the zinc electrolyte purification process of a hydrometallurgical zinc plant through reduction in zinc dust consumption. *Hydrometallurgy* 40:247.

Spedden, H.R., Malouf, E.E., and Prater, J.D. 1966. Cone-type precipitators for improved copper recovery. *J. Met.* 18(10):1137.

Straumanis, M.E., and Fang, C.C. 1951. Structure of metal deposits obtained by electrochemical displacement upon zinc. *J. Electrochem. Soc.* 98(1):9.

Strickland, P.H., and Lawson, F. 1971. The cementation of metals from dilute aqueous solution. *Proc. Aust. Inst. Min. Met.* 237:71.

Strickland, P.H., and Lawson, F. 1973. The measurement and interpretation of cementation rate data. In *International Symposium on Hydrometallurgy*. Edited by D.J.I. Evans and R.S. Shoemaker. New York: AIME.

Taha, A.A., and Ghani, S.A. 2005. Effect of surfactants on the cementation of cadmium. *J. Colloid Interface Sci.* 280(1):9.

Von Hahn, E.A., and Ingraham, T.R. 1966. Kinetics of PdII cementation on sheet copper in perchlorate solutions. *Trans. Metall. Soc. AIME* 236:1098.

Younesi, S.R., Alimadadi, H., Alamdari, E.K., and Marashi, S.P.H. 2006. Kinetic mechanisms of cementation of cadmium ions by zinc powder from sulphate solutions. *Hydrometallurgy* 84:155.